A REVIEW ON METAL ION DOPED SnO_2 NANOCOMPOSITES: SYNTHESIS AND APPLICATION IN PHOTOCATALYTIC DEGRADATION AND ANTIMICROBIAL ACTIVITIES

Abstract

Photocatalysis is the speeding up of the photoreaction in the prevalence of light. The most common heterogeneous photocatalysts are transition metal oxides and certain semiconductors. Among the transition metal oxides TiO_2, ZnO and SnO_2 are low-cost materials with good chemical and thermal stability, large surface area, high adsorption properties, less resistance to diffusion, and show faster rates of equilibrium. The study of SnO_2 in the field of photocatalysis is due to its different morphologies, high photochemical stability, strong oxidizing power, low cost, and non-toxic nature. This paper outlines the synthesis of SnO_2 by various techniques with different surface structures and reviews the synthesis of SnO_2 nanoparticles in connection with enhanced photodegradation and antibacterial efficacy.

Keywords: SnO_2 nanoparticles, photocatalysis, antimicrobial activities

Authors

Nirmala B
Department of Studies and Research in Chemistry
University College of Science
Tumkur University
Tumakuru, Karntaka, India.
nirmala2528@gmail.com

Bhagyalakshmi M
Department of Biochemistry
University College of Science,
Tumkur University
Tumakuru, Karntaka, India.
bhagyaayanur@gmail.com

I. INTRODUCTION

Metal and non-metallic characteristics are present in semiconductor Nps. They have wide band gaps and displayed significant alteration in their properties. Therefore, they are very significant materials in photocatalysis, photo optics, and electronic devices. Metal oxides are a widely explored and studied class of inorganic solids due to a wide variety of structures, properties, and exceptional phenomena exhibited by their Nps. Metal ions bind with oxides to generate metal oxides (MO), which result in a densely packed structure. MO is a significant player in the field of material research because of its exceptional physical and chemical characteristics. Numerous industrial applications have made use of transition metal oxides. Metal oxides are frequently found and exist in a variety of forms with unique compositions, structures, and chemical and physical characteristics [1]. Some examples are TiO_2, ZnO, SnO_2, VOx, MoOx, and other well-known MO.

Tin oxide (SnO_2) is one of the most attractive and promising materials among metal oxides. This makes SnO_2 a promising candidate for potential use in lithium-ion batteries, sensors, catalysis, field emission displays[2], light-emitting diodes[3], dye-based solar cells[4], energy storage, glass coatings, medicine, environmental remediation[5-8], transistors, optoelectronics devices, solar cells, supercapacitors[9-13], support for catalysts, transparent conducting electrodes[14], antireflective coatings[15], and material for metal oxide sensors in prototype form [16]. SnO_2 is used as a sensor because it has a high specific area, great chemical stability, low electrical resistance, low density, accelerating response time and, increasing sensitivity [17].

The most prevalent heterogeneous photocatalysts are semiconductors and d-block metal oxides. TiO_2, ZnO, and SnO_2 are three transition metal oxides that are inexpensive, have good chemical and thermal stability, a wide surface area, strong adsorption capabilities, little resistance to diffusion, and exhibit quicker rates of equilibrium [18]. SnO_2 has a wide range of morphologies, a high degree of photochemical stability, a potent oxidizing capability, is inexpensive, and is non-toxic, all of which make it a valuable photocatalyst [19].

In this review, pure SnO_2 hierarchical structure synthesis methodologies and performance improvement techniques were discussed. The use of SnO_2-based nanostructures' in photodegradation and antibacterial processes is also discussed. The addition of metal ions, or noble metals to SnO_2 can moderately increase the separation efficiency of photoexcited (e/h+), enhancing the photocatalytic assets for future research.

SnO_2 NPs were prepared using a variety of physical, chemical, and environmentally friendly techniques (Fig. 1). The chemical techniques comprise sol-gel, hydrothermal, precipitation, mechanochemical process, microemulsion, and others [20]. The most common chemical procedure is called sol-gel synthesis, which uses chemical reagents and a salt of a tin precursor to regulate the growth of the gel that contains tin.

The gel is then subjected to heat treatment at a temperature of 800°C to produce SnO_2 NPs. In order to regulate the size and prevent agglomeration of the nanoparticles, chemical stabilizers, and capping agents were used during the synthesis of SnO_2 NPs. The magnitude and morphology of nanoparticles are influenced by the pH, chemical concentration, reaction duration, and calcination temperature [21]. The procedures for making SnO_2 NPs mentioned above include the use of hazardous chemical reagents, solvents, and surfactants that pose a major risk to the atmosphere and public well-being.

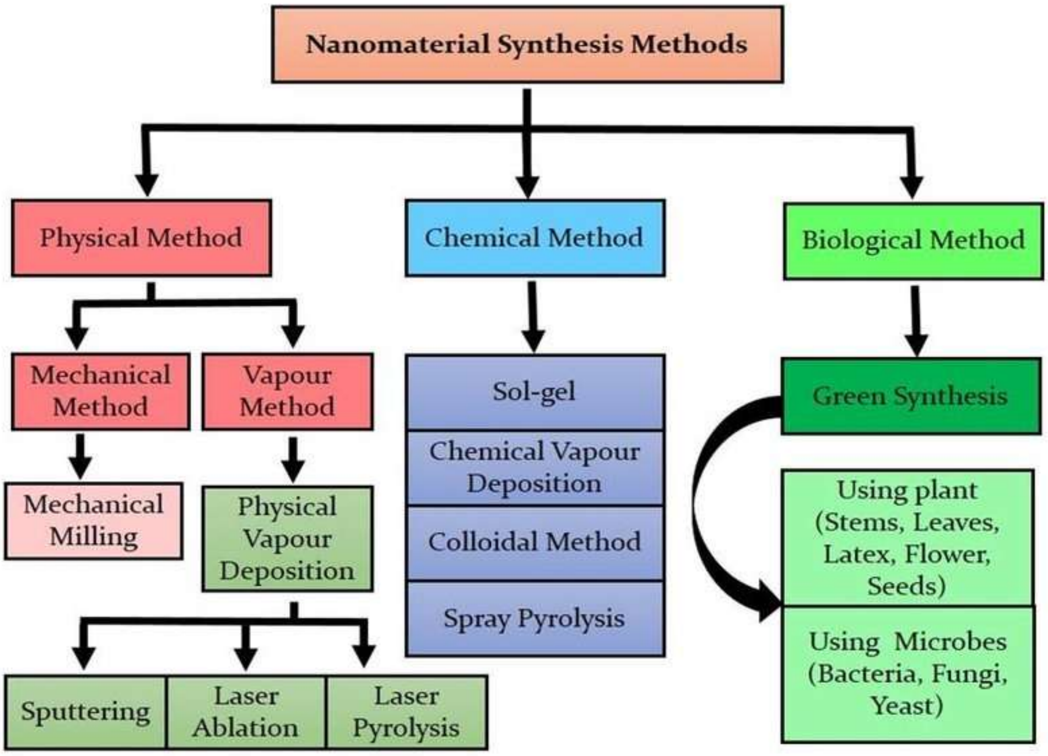

Figure 1: Synthesis Methods for Nanoparticles [22]

In the green synthetic approach, biotic components such as plant extract, microorganisms, or other environmentally friendly sources might be used instead of traditional physical and chemical processes. Biological synthesis (Fig. 2) has certain specific advantages over physical and chemical approaches, including (a) using nontoxic chemicals, which is a clean and environmentally benign process; (b) using renewable resources. (c) The biologically active elements, such as the enzyme itself and phytochemicals, serve as reducing and plugging agents, lowering the overall cost of the manufacturing process [22].

Efforts have been made to create SnO2 nanocomposites with a variety of surface characteristics, including nanorods, nanowires, nanotubes, nanosheets, and 3D nanospheres that self-assembled from these low-dimensional nanostructures with interactions like van der Waals forces, hydrogen, and covalent bonding. (Fig 3).

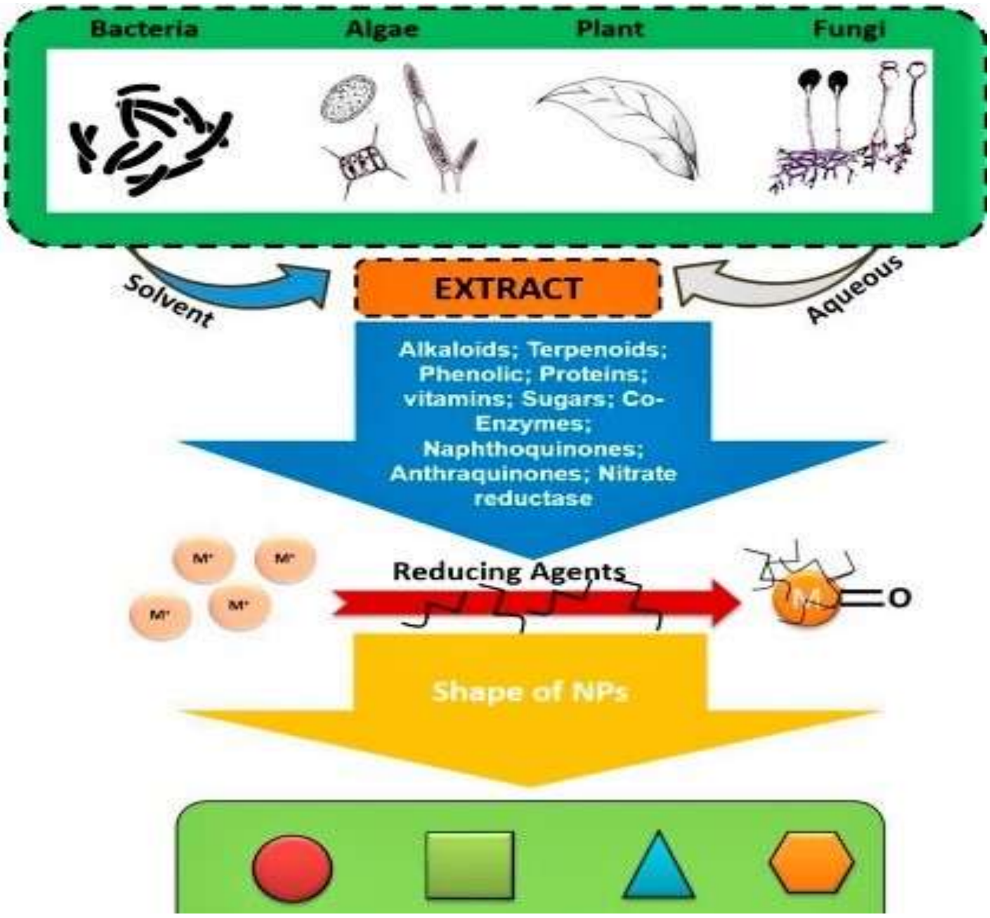

Figure 2: Synthesis of Nanoparticles Using Different Biological Sources [29]

By doping SnO2 NPs with d-block elements [26-32], numerous attempts have been made to increase the photosensitivity of SnO2 throughout the electromagnetic spectrum. The photocatalytic activity is additionally increased by the addition of different concentrations of these dopant species. Broad energy band gap prevents this photo activation and sites for electron-hole recombination can be provided by increasing doping content [33].

Different characterization techniques have been practiced for the investigation of various physicochemical properties of NPs. These techniques include X-Ray Diffraction (XRD), X-Ray Photoelectron Spectroscopy (XPS), Infrared Spectroscopy (IR), Scanning Electron Microscopy (SEM), Transmission Electron Microscopy (TEM), absorption Spectroscopy, PL studies, Brunauer–Emmett–Teller (BET) and Particle size analysis (Fig.4) [34]. Finally, the photodecomposition was studied by using pure and metal incorporated SnO2 nanoparticles as a catalytic agent under UV/visible light irradiation, and antimicrobial assay was evaluated and their performances were reviewed.

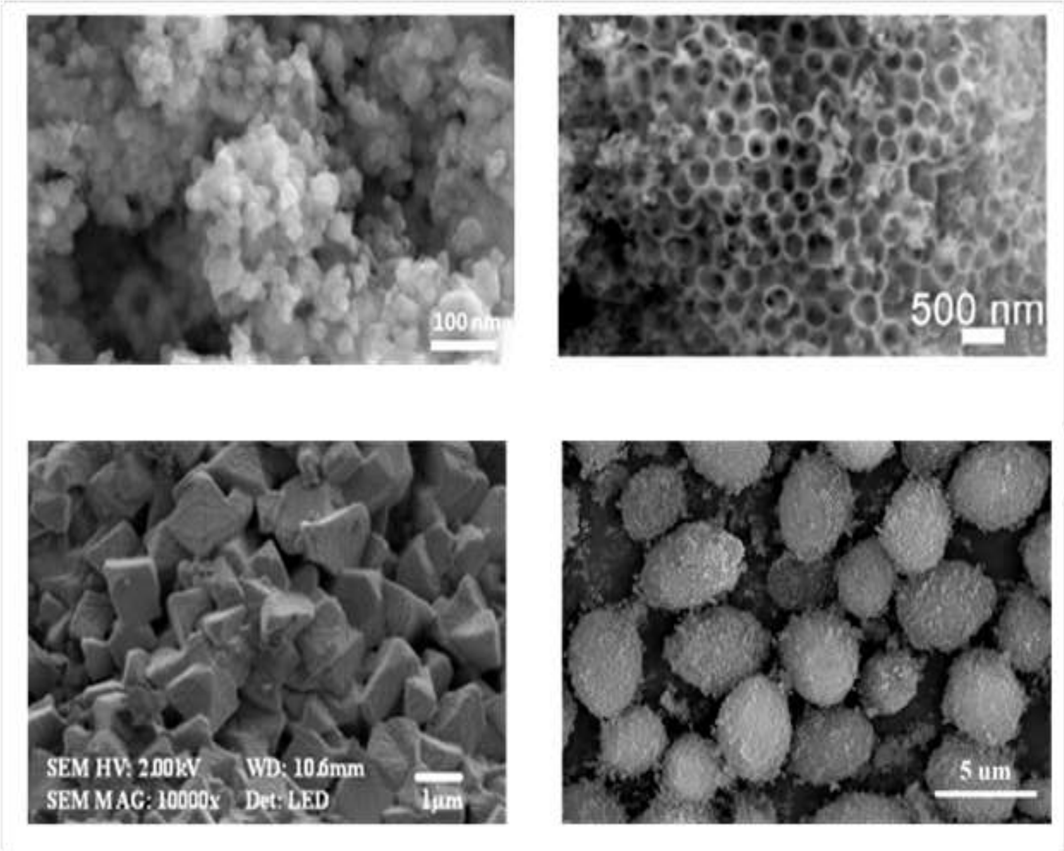

Figure 3: SEM Images Showing Different Morphologies Of Nps[36,37]

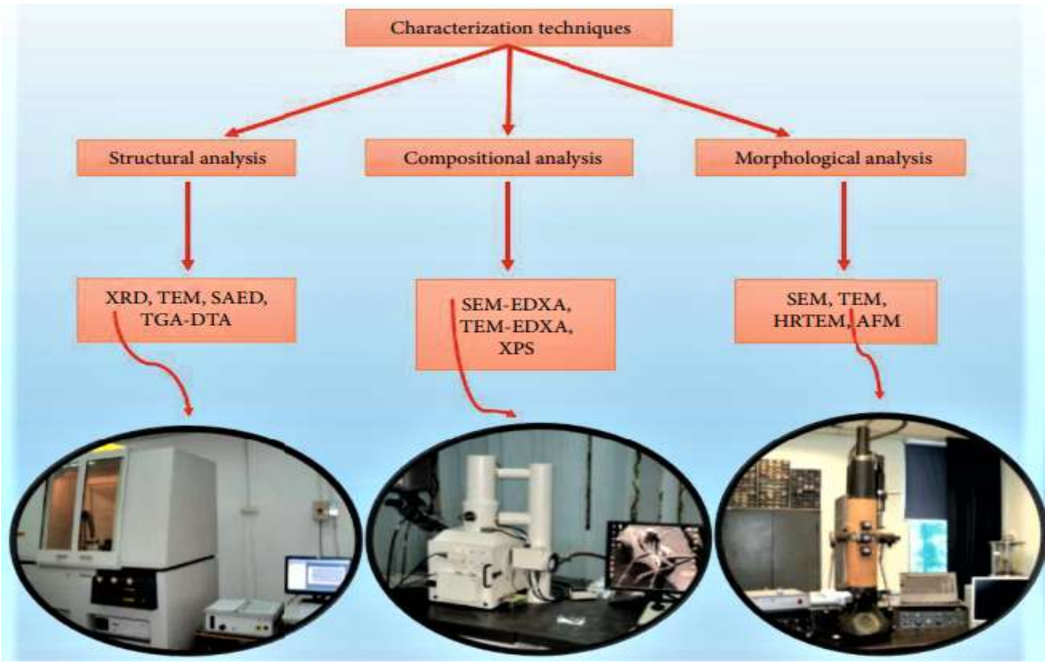

Figure 4: Techniques for Identifying Nanoparticles [34]

Sn-containing fluoride compound, $KSnF_3$ was used as the single-source precursor in the effective preparation of F-doped SnO_2 nanocrystals by Kumar, V. et al. [38]. Powder X-ray diffracted peaks revealed the low crystallite size, which was allocated to a tetragonal unit cell. EDAX analysis revealed the presence of fluoride ions. The BET surface area of Fluorine-doped SnO_2 nanocrystals was considerably lower (45.16 m2/g) than that of undoped SnO_2 (207.81 m2/g). F-doped SnO_2 nanocrystals were shown to have extremely high photocatalytic effectiveness when compared to pure SnO_2.

Super symmetric nanocomposites with a high superficial area of hollow Au-SnO_2 were formed by a solvothermal reaction using DMF solvent in the presence of capping agents by You, H et al. [40]. This work showed that the preliminary formation of ultrafine SnO_2 nanoclusters accumulated to form hollow hexapods.

By using a seed-mediated hydrothermal technique, Wu, W. et al. [41] created hollow SnO_2-Au hybrid nanostructures, and the development of their form was studied (Fig. 5). With lattice constants of a = 4.738 and c = 3.187, XRD patterns displayed rutile tin oxide phase strong peaks and weak gold peaks. EDAX studies confirmed the presence of Au, Sn, and O.

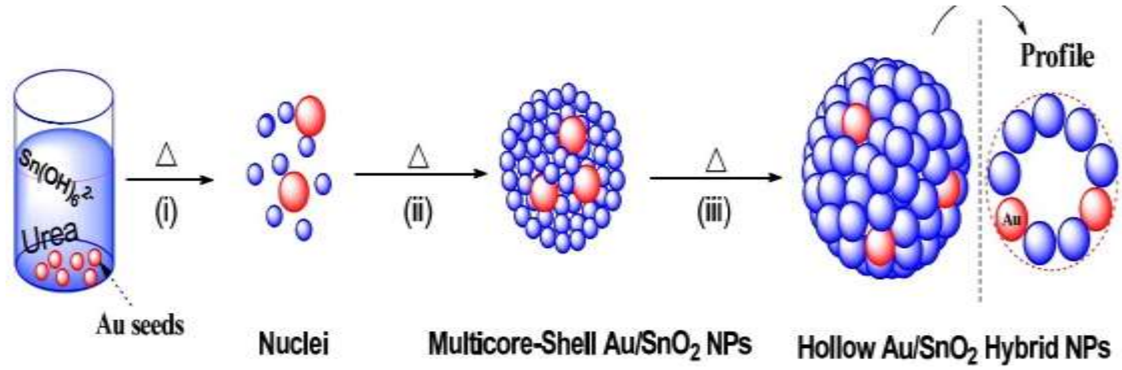

Figure 5: Schematic Representation of the Formation of Hollow SnO_2-Au Hybrid Nanostructures [41]

A modest sol-gel approach was used to produce fine iron-doped SnO_2 nano architectures with effective photocatalytic removal of water-soluble dyes under electromagnetic irradiation by Davis, M. et al. [42]. All the materials were annealed at 350^0C. The presence of iron was confirmed by EDAX.

Using an EAB free of hazardous substances, surfactants, and organic solvents, Ansari, S. et al. [43] created Ag-SnO_2 nanocomposites with various concentrations of silver precursor (1 mM and 3 mM) at ambient temperature. Ag-SnO_2 nanocomposites displayed a large absorption peak between 400 and 550 nm, which was attributed to AgNPs' surface plasmon resonance absorption. Ag-SnO_2 nanocomposites demonstrated improved photocatalytic activity in comparison to pure SnO_2 under visible light for the degradation of cationic and anionic dyes and nitrophenols.

Tin chloride dihydrate, cobalt chloride hexahydrate, sodium hydroxide, and ethanol were used in the chemical precipitation process by Toloman, D. et al. [44] to create a variety of Cobalt-doped SnO_2 nanoparticles. An increase in the level of doping increase in the samples' crystallinity was observed. Under the influence of visible light, the sample's photocatalytic activity was assessed.

Using SiO_2 microspheres as hard templates, Ran L. et al. [45] used a simple infiltration technique for manufacturing hollow-structured SnO_2 with a variable Titanium doping concentration. Titanium doping had no effect on the samples' crystal structure or morphology, and they maintained their highly crystalline condition and hollow spherical nanostructure with a particle diameter of roughly 300 nm.

Zn-doped SnO_2 hierarchical structures (ZSHAs) of controlled size were created by Zhao, Q. et al. [46] using a simple hydrothermal technique, and they were made of two-dimensional (2D) nanosheets with a thickness of about 40 nm. The crystal was identified by the XRD pattern. TEM examination revealed nanosheet structures. The nanosheet structures' composition of Zinc, tin, and Oxygen components was revealed by EDAX analysis. Both cationic and anionic dyes were used for degradation to assess the photocatalytic activity of ZSHAs.

Using an electrochemically active biofilm, Khan, M. M. et al. [47] produced Au-SnO_2 nanocomposite. XRD results were further supported by a Reitfield refinement. The visible part of the spectrum of the Au-SnO_2 nanocomposite displayed a wide absorption peak between 500 and 600 nm, which was attributed to the surface plasmon resonance absorption of the Au NPs. XPS was used to analyze the surface chemistry and chemical conditions of Au-SnO_2 nanocomposite and P-SnO_2 nanoparticles. In comparison to P-SnO_2 nanoparticles, the Au-doped SnO_2 nanocomposites showed remarkably enhanced photocatalytic activity.

By using the sol-gel process, Chandran, D. et al. [48] successfully synthesized pure and cobalt-doped SnO_2 nanoparticles with varying cobalt concentrations (0.75, 3, and 4 at%). When the cobalt concentration was increased, it was found that the diffraction peaks widened and the crystallinity decreased in comparison to pure SnO_2. The samples that have been doped showed an additional peak between 375 and 505 nm when compared to pure SnO_2. The degradation of methylene blue solution in the presence of natural light was used to assess the photocatalytic effectiveness of pure and doped samples.

SnO_2 and Co-doped SnO_2 nanoparticles were successfully produced by Sivakarthik, P. et al. [49] using the organic solvent-assisted simple solution approach and calcined at 300–500^0C. In the presence of Co-doped SnO_2 at various concentrations, photocatalytic degradation of synthetic organic dye Crystal violet has been studied.

Mani, R et al. [50] also synthesized pure and Co-doped SnO_2 nanoparticles by simple chemical precipitation method. Powder XRD results revealed that both pure and Co-doped SnO_2 nanoparticles were indexed to a tetragonal rutile-type structure. Under UV illumination, a Co-SnO_2 catalyst was used to study the photocatalytic oxidation of carbolic acid and phenyl formic acid. In comparison to pure SnO_2, the results indicated that Co-doped SnO_2 had the strongest photo-catalytic abilities.

Iron-doped tin dioxide nanoparticles ($Sn_{1-x}Fe_xO_2$ NPs), with x ranging from 0 to 0.2, were effectively created by Ben Haj Othman et al. [51] using a conventional hydrothermal process. UV-Vis measurements suggest that adding iron could change the band gap of SnO_2

NPs. Degradation studies show addition of iron to SnO_2 nanoparticles enhances catalytic activity.

By using the polyol method at atmospheric pressure, Soltan, W. B. et al. [52] effectively produced nanocrystalline mesoporous pure and vanadium-doped (0-10 at%) SnO_2 nanopowders using ammonium metavanadate and tin (IV) tetrachloride. As the concentration of vanadium increased, a decrease in mean crystallite size, average pore size, and an increase in surface area were observed.

By using the precipitation process, Sinha, T. et al. [53] successfully manufactured Ag-SnO_2 nanocomposites. TEM studies indicate that Ag-SnO_2 nanocomposites are sphere-shaped particles with an average particle diameter of 8–10 nm. The resulting Ag-SnO_2 nanocomposite was used as an antibacterial and antioxidant agent as well as for the removal of industrially emerging pollutants from the aqueous phase.

Co-doped SnO_2 NPs with an average size of 30–40 nm were successfully created by Nasir, Z. et al. [54] using the co-precipitation approach utilizing $SnCl_2.2H_2O$ and $CoCl_2.2H_2O$ as Sn and Co precursors. The production of the nanoparticles was confirmed by XRD and SEM.

By utilizing an easy and affordable co-precipitation technique, Qamar, M. A. et al. [55] were able to successfully synthesize Cobalt-doped SnO_2 nanoparticles. The energy gap was further reduced when these SnO_2 were Co-doped. Undoped SnO_2 nanoparticles had a band gap of 3.36 eV, and doped SnO_2 nanoparticles had a band gap of 1.48 eV. Inhibition zone (mm) experiments show that Co-doped SnO_2 nanoparticles have antibacterial activity against the selected microorganisms.

By using a chemical precipitation approach and 500°C annealing, Karpuraranjith, M., et al. [56] were able to successfully synthesize a biotemplate-zinc-tin oxide hybrid structure. The unique rutile structure of SnO_2 with average crystalline sizes of 1.54–9.01 nm was revealed by the X-ray diffraction peaks. The hybrid structure's optical band gap energy was determined to be 3.19 eV. Zinc-tin oxide hybrid structure based on a bio template emerged as a suitable component for photocatalytic degradation.

Pristine and (Mg+Co) doped tin oxide nanoparticles were effectively made by Mala, N. et al. [57] using a wet chemical process. XRD pattern of the (Mg+Co) doped SnO_2 nanoparticles matched with the undoped SnO_2 nanoparticles suggests that the doped nanoparticles also exhibited a rutile hexagonal structure. The antibacterial and photocatalytic properties of the material were caused by the presence of hydroxyl groups.

Using $SnCl_2$, $MnCl_2$, and triethanolamine, Sakwises, L. et al. [58] successfully synthesized SnO_2 and Mn-doped SnO_2 nanoparticles. 40% wt of Mn was entirely substituted, according to FT-IR and XRD. The photocatalytic activity on the breakdown of methylene blue was studied to determine the effectiveness of SnO_2 and Mn-doped SnO_2.

By using a microwave irradiation technique and attaching it to the surface of Silk fibroin (SF), Bhuvaneswari, K. et al. [59] successfully synthesized pure SnO_2, and Cd / Zn-doped SnO_2 nanopowders. The lowering crystallite size increased active surface area, and reduced particle distribution after connecting SF. all contributed to the increase in photocatalytic activity. Zn-doped SnO_2 photocatalyst with SF links exhibited more dye degradation.

Efficient quantum dots of Tin oxide with different concentrations of Manganese were effectively produced through green synthesis by Babu, B. et al. [60]. X-ray diffraction patterns were used to analyze the structural characteristics of the undoped and Mn-doped SnO_2 QDs. Under visible light, Mn-doped SnO_2 QDs were used as a catalytic agent to test the photodegradation of cationic dye.

Using the co-precipitation approach, Asaithambi, S. et al. [61] produced pure and cobalt (Co)-doped SnO_2 nanoparticles successfully. EDAX results showed the presence of tin, oxygen, and cobalt species. Catalytic activities of pure and Cobalt-doped SnO_2 nanoparticles were investigated by photodegradation of green dye, an organic contaminant.

The co-precipitation approach was used by Sujatha, K. et al. [62] to manufacture and analyze pure, zinc-doped, and surfactant-assisted Zn-doped SnO_2 NPs. The band gap values calculated from Tauc's plot for the Zn-doped SnO_2 nanoparticles showed a significant change from 3.292 eV to 3.695 eV. The highest photocatalytic activity (80%) and best optical characteristics were obtained in Zn-doped SnO_2 nanoparticles produced with triton assistance. In contrast to TRITON-assisted Zn-doped SnO_2 NPs, pure, CTAB- and SDS-assisted Zn-doped SnO_2 NPs exhibit a very high rate of photogenerated electron-hole pair (e, h+) recombination, which inhibits the generation of the hydroxyl radical.

By co-precipitation process, varying the concentration of vanadium from 0% to 4%, Letifi, H. et al. [63] synthesized vanadium-doped SnO_2 nanoparticles. It is observed that the absorption edge shifted toward the red with an increase in vanadium concentration. The optical band gap decreased as a result of this redshift from 3.25 eV to 2.55 eV. Compared to SnO_2 NPs, SnO_2:V NPs showed an enhanced photocatalytic reaction.

The increased antibacterial and photocatalytic activity of pure and copper-doped SnO_2 nanoparticles was successfully investigated by Sathish Kumar, M et al. [64] using the microwave-assisted technique. The synthesis of NPs used tin chloride dihydrate ($SnCl_2.2H_2O$) and copper chloride hexahydrate ($CuCl_2.6H_2O$) as tin and copper sources respectively. Optical properties were explored by UV visible and Photoluminescence spectroscopy. Copper-doped SnO_2 nanoparticles showed an excellent zone of inhibition against both pathogens. Under UV light, photocatalytic degradation abilities for the cationic dyes were also assessed.

Sujatha, K. et al. [65] used tin chloride dihydrate and ferric chloride as precursors with ethanol and ammonia to successfully synthesize Iron-doped and surfactant-assisted (CTAB, SDS, and Triton) Iron-doped SnO_2 NPs. The addition of iron and surfactants was found to increase the band gap. The photocatalytic analysis confirmed that undoped SnO_2 NPs showed considerable photocatalytic activity under visible light.

Tin chloride ($SnCl_2.5H_2O$; 98%), ethanol (C_2H_5OH), iron chloride ($FeCl_2.5H_2O$; 98%), and sodium hydroxide (NaOH; 99%) were used in the preparation of undoped and iron-doped tin SnO_2 nanoparticles by Ali Baig et al. [66]. Due to the Fe dopant's nominal defect, the intensity will be reduced. Degradation studies show Fe-doped SnO_2 NPs had more photocatalytic activity than pure SnO_2. The synthesized nanoparticles exhibit exceptional antibacterial activity.

Using $SnCl_2.2H_2O$, $FeCl_3.6H_2O$, aqua ammonia, and urea as raw materials, Wang, Q et al. [67] synthesized novel material Fe (1, 2, and 3 wt%) doped SnO_2 adorned layered g-C_3N_4 using a chemical precipitation technique. The as-prepared hybrid material 1wt% Fe-SnO_2/g-C_3N_4 (1 wt% Fe-SCN) showed improved activity of photodegradation under simulated solar light irradiation.

By chemically precipitating stannous chloride, Ethane dioic acid, and Manganese diacetate tetrahydrate, Ramamoorthy M. et al. [68] created Manganese-doped SnO_2. Manganese doped tin oxide shows less band gap than undoped one and an improved size, and superficial area.

Suthakaran, S et al. [69] successfully prepared Zr-doped SnO_2 NPs by surfactant-assisted hydrothermal method using Tin (IV) chloride pentahydrate ($SnCl_4.5H_2O$), Zirconyl chloride octahydrate ($ZrOCl_2.8H_2O$), caustic acid (NaOH), and sodium polymetaphosphate. The results of XRD confirmed the simple, polycrystalline nanoparticles with a tetragonal structure and remained stable even after higher concentrations of Zirconium dopant. Photocatalytic measurements showed that doped NPs improved the photodegradation percentage of the MV dye.

According to Baig, A. et al. [70], nanocrystalline pristine and zirconium-incorporated tin oxide NPs were prepared by simple hydrothermal co-precipitation mode. A detailed investigation of the photodegradation capabilities of 4% doped tin oxide nanoparticles (NPs) was studied under visible light. In comparison to undoped SnO_2, doped NPs photo-catalytically are more capable and show good antibacterial activity against E. coli and S. aureus bacteria.

Using a hydrothermal chemical process with varying Y doping concentrations (0, 2, and 4 at%), Baig, A. et al. [71] successfully produced SnO_2 NPs. Both pure and yttrium-doped NPs show tetragonal crystalline texture. XRD studies show the size decreased after Y^{3+}doping. HRSEM showed equivalent crystallite spreading and agglomeration morphologies. Even after five cycles, the yttrium-doped nanoparticles showed efficient photodegradation.

In-SnO_2 nanomaterial was produced by Carolin, L. et al. [72] by precipitation and sonication. UV absorption studies were carried out to determine the band gap of both pure and indium-doped nanoparticles. SnO_2 photo catalyst confirmed the catalyst's excellent reusability characteristics. Hydroxyl Radical production is directly associated with the photocatalytic activity of In-SnO_2 nanocomposite. In-doped SnO_2 has greater antibacterial activity than undoped SnO_2.

Bi-doped SnO_2 quantum dots were made using hydrothermal synthesis in a single step by Chu, L. et al. [73]. Under visible light, the efficiency of the photocatalyst was assessed. The resulting composites displayed outstanding photodegradation efficiency because of enhanced light absorption and the effective parting and movement of photo-generated electrons.

Using a high-temperature oxy-acetylene flame, Prabhu et al. [74] created pure SnO_2 and Zn: SnO_2 nanoparticles. Nano cubical and nanoflake Zn: SnO_2 nanoparticles with an improved crystalline structure replace irregular, agglomerated, nanoflowers, and nano clustered SnO_2 nanoparticles. Due to the production of highly reactive (OH-) hydroxyl and superoxide (O^{2-}) radicals, both doped and undoped SnO_2 nanoparticles show excellent photocatalytic activity under UV light.

By using Populus ciliate leaf extract, Slah Ud Din et al. [75] created SnO_2 nanoparticles. XRD and EDAX studies confirmed the formation of composites. The diffusion technique based on agar wells was used to examine the antibacterial properties.

Table 1: Synthesis of Metal Ion Doped Sno_2-Based Nanostructures: A Summary of Several Techniques

Authors and Year	Sample	Synthesis Route	Structural Characterization	Results	Ref.
Kumar, V et al. (2011)	F- SnO_2	sol-gel method	PXRD (a = 4.7106 Å & c = 3.1970 Å), TEM, BET, Raman spectrum, EDX, Pore size analysis.	Increased photocatalytic efficiency in the degradation of aqueous Rhodamine-B (RhB) dye solution under UV irradiation.	39
You, H et al. (2013)	Au–SnO_2	solution reaction	XRD(rutile-type), SEM, TEM, SAED, BET.	Improves photodegradation	40
Wu, W et al. (2013)	Au–SnO_2	hydrothermal method	XRD (crystallite sizes 10.8 nm), HRTEM, BET, EDX, BET pore size(16.8 nm), UV-DRS	improved photocatalyt c degradation of RhB under UV and visible light irradiation.	41
Davis, M et al. (2013)	Fe-SnO_2	sol–gel method	XRD(3nm), Gas sorption analyses, Electron microscopy studies, Pore size analysis, EDX	Enhanced photocatalytic performance under UV light.	42

Ansari, S et al. (2014)	Ag–SnO2	EAB (electrochemically active biofilm).	XRD, surface plasmon resonance absorption(400–550nm)	Increased photocatalytic activity for the breakdown of methyl orange and methylene blue when exposed to visible light.	43
Toloman, D et al. (2014)	Co - SnO_2	chemical precipitation method	XRD (tetragonal rutile), EPR.	Under visible light irradiation, the sample's photocatalytic activity was assessed against a synthetic RhB solution.	44
Ran, L et al. (2015)	Ti-SnO_2	facile infiltration route	XRD, BET	Shows highest photocatalytic activity for photodegradation of methylene blue under UV light.	45
Zhao, Q et al. (2015)	Zn-SnO_2	hydrothermal method	XRD (tetragonal rutile structure), SEM(2D nanosheets), EDX.	Photocatalytic degradation of methylene blue (MB-91%), methylene orange (MO-40%), and rhodamine B (RhB-60%) in 60min.	46
Khan, M. M et al. (2015)	Au–SnO_2	electrochemically active biofilm.	XRD (crystallite size is 25–30 nm). UV-Vis(500-600nm), XPS.	Efficient photodegradation of cationic and anionic dyes.	47
Chandra, D et al. (2015)	Co-SnO_2	sol-gel method	XRD (tetragonal rutile-type), HRTEM, UV spectra(375-505nm)	The decomposition of the MB solution under natural light was used to calculate the photocatalytic efficiency.	48

Sivakarthik, P et al. (2016)	Co - SnO_2	simple solution method	XRD (tetragonal structure & particle size of 18 nm to 22 nm)., SEM (spherical morphology)	exhibited high photocatalytic activity for the breakdown of Crystal violet dye.	49
Mani, R et al. (2017)	Co - SnO_2	chemical precipitation method	XRD (tetragonal rutile, average crystalline size 48, 41, and 32 nm), TEM, FTIR, UV-Vis	Under UV irradiation, the degradation of phenol and benzoic acid was studied.	50
Ben Haj Othmen et al. (2016)	Fe- SnO_2	hydrothermal method.	XRD (tetragonal rutile structure), HRTEM, BET, UV-Vis.	Enhanced degradation of RhB under visible light.	51
Soltan, W. B et al. (2016)	V- SnO_2	polyol route	XRD (rutile-type tetragonal structure with average crystallite sizes 8.8 to 5.4 nm), UV-DRS.	Catalytic studies were carried out by varying the concentration of Vanadium.	52
Sinha, T et al.(2016)	Ag-SnO_2	Simple precipitation method	XRD, TEM, EDAX, SAED	Utilized for the reduction of industrially developing pollutants and as an antibacterial agent.	53
Nasir, Z et al. (2017)	Co - SnO_2	co-precipitation method	XRD (tetragonal-rutile type structures), SEM, TEM, SAED	Enhanced catalytic property under UV light and has increased antimicrobial effect.	16
Qamar, M. A et al. (2017)	Co-SnO_2	co-precipitation method.	XRD (tetragonal structure having average crystallite size 24.86 nm), SEM (spherical shape), EDX, UV-Vis.	Improved Antibacterial activities	17

Karpuraranjith, M et al. (2017)	Zn-SnO_2	Chemical precipitation method	XRD(distinctive rutile structure with average crystalline sizes of 1.54–9.01 nm), SEM(cluster), EDAX, TEM(agglomerated), UV-Vis(3.19eV)	Bio-based templates Zn-SnO_2 and is an effective substance for enhancing photocatalytic activity.	18
Mala, N et al. (2017)	(Mg+Co) doped SnO_2	wet chemical method	XRD (rutile hexagonal structure), FT-IR.	For Malachite Green (MG) and MB, the degradation efficiency of pure SnO_2 was 82% and 86%, respectively.	19
Sakwises, L et al. (2017)	Mn-SnO_2	wet chemical synthetic route	FT-IR, XRD, and EDAX.	The degradation of water-soluble dyes under UV irradiation.	20
Bhuvaneswari, K et al. (2018)	Cd / Zn-doped SnO_2	Microwave irradiation method	XRD (rutile-tetragonal system with an average crystallite size 43.4, 22.8, and 24.3 nm), FT-IR, UV-Vis spectra.	Zn-doped SnO_2 nanoparticles' photocatalytic activity showed a remarkable MB degradation efficiency of 99.6%.	21
Babu, B et al. (2018)	Mn-SnO_2	solution combustion	XRD (tetragonal rutile structure with a particle size ranging from 5 to 4.4 nanometer), SAED, FT-IR, UV-Vis.	Removal of water-soluble dye under sunlight	22
Asaithambi,S et al. (2019)	Co-SnO_2	co-precipitation method	XRD (cassiterite tetragonal SnO_2 structure with average crystalline between 26.4 nm and 23.1 nm), FT-IR, UV-Vis, HRTEM, SAED.	Co-doped SnO_2 shows enhanced photocatalytic activity.	23

Sujatha, K et al. (2019)	Zn -SnO_2	co-precipitation method	XRD (rutile tetragonal with crystallite size 9.34 nm), SEM(Spherical), EDAX, UV-Vis.	Better optical characteristics and a high (80%) photocatalytic activity.	24
Letifi, H et al. (2019)	V-SnO_2	co-precipitation method	XRD (tetragonal structure & the average crystal size is 10nm), UV-Vis(55eV)	The photocatalytic degradation has been studied using the Rhodamine B dye (RhB; 95 percent in 150 minutes).	25
Sathishkumar, M et al. (2020)	Cu-SnO_2	microwave assisted method	XRD TEM(Spherical), UV-Vis(3.20eV).	Enhanced antibacterial (P. aeruginosa & S. aureus) and photocatalytic activity (MB, RhB)	26
Sujatha, K et al. (2020)	Fe-SnO_2	co-precipitation method	XRD (tetragonal rutile structure with a crystallite size 6.347 nm), SEM, TEM, EDAX, UV-Vis.	Enhanced degradation of dye (MB) was found to be 49% respectively.	27
Ali Baig et al. (2020)	Fe- SnO_2	co-precipitation method	XRD, HRTEM (agglomerated), UV-DRS.	Higher photocatalytic dye degradation efficiency under visible light and antibacterial activity was determined against E.coli and S.aureus bacteria.	28
Wang, Q et al. (2020)	Fe -SnO_2	simple chemical precipitation method	XRD, HRTEM, EDS, XPS, UV-DRS	Enhanced photocatalytic activity and photodegradation of methylene blue and rhodamine B in the presence of simulated solar light.	29

Ramamoorthy, M et al. (2020)	Mn-SnO_2	chemical precipitation method	XRD (rutile tetragonal structure, crystallite size 13.79nm), UV-Vis	Studies on the degradation of methylene blue dye under visible light were carried out..	30
Suthakaran, S et al. (2020)	Zr -SnO_2	hydrothermal method	XRD, TEM, PL.	Photocatalytic measurements showed that doped NPs improved the photodegradation percentage of the MV dye.	31
Baig, A et al. (2020)	Zr-SnO_2	facile hydrothermal co-precipitation	XRD (tetragonal rutile-type), SEM, EDX, UV-DRS	increased photocatalytic degradation and antibacterial activity.	32
Baig, A et al. (2020)	Y-SnO_2	hydrothermal chemical route	XRD,SEM(agglomeration), UV-DRS	Enhanced photodegradation of cationic dye in apparent light, enhanced antibacterial activity	33
Carolin, L et al. (2020)	In–SnO_2	precipitation method and sonication technique	XRD (cassiterite structure and average size of 40–50 nm & 60–80 nm) HRTEM, EDAX, UV-DRS	improved antibacterial activity against B. subtilis and V. cholera and photocatalytic activity under UV light.	34
Chu, L et al. (2020)	Bi-SnO_2	hydrothermal method	XRD XPS, BET, Pore volume analysis.	photocatalytic degradation and antibacterial studies.	35
Sivarama Prabhu P (2021)	Zn: SnO_2	Flame oxidation process	XRD, FT-IR	Photocatalytic degradation of cationic dye	74
Salah Ud Din etal [2022]	SnO_2	biosynthesis	The FT-IR and TGA	Antibacterial studies were carried out	75

II. CONCLUSIONS

This review covered the formation of SnO_2 hierarchical structures, their doping and compositional modifications, as well as the creation of stannate nanomaterials with various morphologies, such as nanoparticles, nanorods, nanosheets, nanospheres, and porous and hollow structures. Tin oxide nanomaterials have been expected to be powerful photocatalysts for the degradation of organic pollutants in aqueous solution due to their excellent properties such as transparency, low cost, environmental friendliness, good chemical and biological inertness, nontoxicity, easy production and high photosensitivity, photostability, and thermodynamic stability. Tin oxide is also known for its antimicrobial activity especially antibacterial properties against many gram-positive and gram-negative bacteria.

The high activation energy of the metal oxide limits the experimental use of SnO_2 semiconductors as a pure material, despite their excellent promise for photo-catalytic applications and their antioxidant activity against free radicals. This activation energy corresponds to UV light exposure and the direct (rapid) recombination rate of the photo-generated conduction electron (e CB) in the Sn 4d(5S) band and with a hole in the O 2p valence band. The rate of electron-hole pair recombination needs to be suppressed in order to improve the industrial use of SnO_2 and boost the photo-catalytic activity. Doping other semiconductors with metal oxides that have different band gaps for electron energies is one method. The new combination material's photo-catalytic activity might then be enhanced as a result of the reduced activation energy.

SnO_2-based nanomaterial gained widespread usage after the addition of components with various chemical compositions. It is still difficult and challenging to synthesize SnO_2 nanocrystals on a wide scale with more specialized aspects. Future advancements will be made and novel intriguing Nano systems will produce the technologies in the synthesis of nanostructures to precisely control dimension and composition.

REFERENCES

[1] Nair, M. G., Nirmala, M., Rekha, K., & Anukaliani, A. (2011). Structural, optical, photocatalytic, and antibacterial activity of ZnO and Co-doped ZnO nanoparticles. Materials Letters, 65(12), 1797-1800
[2] Li, L., Zong, F., Cui, X., Ma, H., Wu, X., Zhang, Q., & Zhao, J. (2007). Structure and field emission properties of SnO_2 nanowires. Materials Letters, 61(19-20), 4152-4155
[3] Wang, Y., & Chen, T. (2009). Nonaqueous and template-free synthesis of Sb doped SnO_2 microspheres and their application to lithium-ion battery anode. Electrochimica Acta, 54(13), 3510-3515.
[4] Snaith, H. J., & Ducati, C. (2010). SnO_2-based dye-sensitized hybrid solar cells exhibiting near unity absorbed photon-to-electron conversion efficiency. Nano letters, 10(4), 1259-1265.
[5] Branci, C., Benjelloun, N., Sarradin, J., & Ribes, M. (2000). Vitreous tin oxide-based thin film electrodes for Li-ion micro-batteries. Solid State Ionics, 135(1-4), 169-174.
[6] Hong, Z. R., Liang, C. J., Sun, X. Y., & Zeng, X. T. (2006). Characterization of organic photovoltaic devices with indium-tin-oxide anode treated by plasma in various gases. Journal of applied physics, 100(9), 093711.
[7] Pandey, P. C., Upadhyay, B. C., Pandey, C. M. D., & Pathak, H. C. (1999). Electrochemical studies on D96N bacteriorhodopsin and its application in the development of photosensors. Sensors and Actuators B: Chemical, 56(1-2), 112-120.
[8] Tazikeh, S., Akbari, A., Talebi, A., & Talebi, E. (2014). Synthesis and characterization of tin oxide nanoparticles via the Co-precipitation method. Materials Science-Poland, 32(1), 98-101.

[9] Courtel, F. M., Baranova, E. A., Abu-Lebdeh, Y., & Davidson, I. J. (2010). In situ polyol-assisted synthesis of nano-SnO_2/carbon composite materials as anodes for lithium-ion batteries. Journal of Power Sources, 195(8), 2355-2361.

[10] Pradel, K. C., Ding, Y., Wu, W., Bando, Y., Fukata, N., & Wang, Z. L. (2016). Optoelectronic properties of solution-grown ZnO np or pn core–shell nanowire arrays. ACS Applied Materials & Interfaces, 8(7), 4287-4291.

[11] Chopra, K. L., Major, S., & Pandya, D. K. (1983). Transparent conductors status review. Thin solid films, 102(1), 1-46.

[12] Cojocaru, L., Olivier, C., Toupance, T., Sellier, E., & Hirsch, L. (2013). Size and shape fine-tuning of SnO_2 nanoparticles for highly efficient and stable dye-sensitized solar cells. Journal of Materials Chemistry A, 1(44), 13789-13799.

[13] Mishra, Y. K., Modi, G., Cretu, V., Postica, V., Lupan, O., Reimer, T., & Adelung, R. (2015). Direct growth of freestanding ZnO tetrapod networks for multifunctional applications in photocatalysis, UV photodetection, and gas sensing. ACS applied materials & interfaces, 7(26), 14303-14316.

[14] Harrison, P. G., & Willett, M. J. (1988). The mechanism of operation of tin (IV) oxide carbon monoxide sensors. Nature, 332(6162), 337-339.

[15] He, Y. S., Campbell, J. C., Murphy, R. C., Arendt, M. F., & Swinnea, J. S. (1993). Electrical and optical characterization of Sb: SnO_2. Journal of Materials Research, 8(12), 3131-3134.

[16] Semancik, S., & Fryberger, T. B. (1990). Model studies of SnO_2-based gas sensors: vacancy defects and Pd additive effects. Sensors and actuators B: chemical, 1(1-6), 97-102.

[17]] Wang, S. C., & Shaikh, M. O. (2015). A room temperature H_2 sensor fabricated using high-performance Pt-loaded SnO_2 nanoparticles. Sensors, 15(6), 14286-14297.

[18] Rashad, M. M., Ismail, A. A., Osama, I., Ibrahim, I. A., & Kandil, A. H. T. (2014). Photocatalytic decomposition of dyes using ZnO doped SnO_2 nanoparticles prepared by solvothermal method. Arabian Journal of Chemistry, 7(1), 71-77.

[19] Rana, S., Srivastava, R. S., Sorensson, M. M., & Misra, R. D. K. (2005). Synthesis and characterization of nanoparticles with magnetic core and photocatalytic shell: anatase TiO_2–$NiFe_2O_4$ system. Materials Science and Engineering: B, 119(2), 144-151.

[20] Chakravarty, R., Chakraborty, S., Shukla, R., Bahadur, J., Ram, R., Mazumder, S., & Dash, A. (2016). Mechanochemical synthesis of mesoporous tin oxide: a new generation nano sorbent for 68 Ge/68 Ga generator technology. Dalton Transactions, 45(34), 13361-13372.

[21] Farrukh, M. A., Tan, P., & Adnan, R. (2012). Influence of reaction parameters on the synthesis of surfactant-assisted tin oxide nanoparticles. Turkish Journal of Chemistry, 36(2), 303-314.

[22] Gebreslassie, Y. T., & Gebretnsae, H. G. (2021). Green and Cost-Effective Synthesis of Tin Oxide Nanoparticles: A Review on the Synthesis Methodologies, Mechanism of Formation, and Their Potential Applications. Nanoscale Research Letters, 16(1), 1-16.

[23] Chen, S., Wang, M., Ye, J., Cai, J., Ma, Y., Zhou, H., & Qi, L. (2013). Kinetics-controlled growth of aligned mesocrystalline SnO_2 nanorod arrays for lithium-ion batteries with superior rate performance. Nano Research, 6(4), 243-252.

[24] Dai, Z. R., Gole, J. L., Stout, J. D., & Wang, Z. L. (2002). Tin oxide nanowires, nanoribbons, and nanotubes. The Journal of Physical Chemistry B, 106(6), 1274-1279.

[25] Zhang, J., Guo, J., Xu, H., & Cao, B. (2013). Reactive-template fabrication of porous SnO_2 nanotubes and their remarkable gas-sensing performance. ACS applied materials & Interfaces, 5(16), 7893-7898.

[26] Li, X., Meng, X., Liu, J., Geng, D., Zhang, Y., Banis, M. N., ...& Verbrugge, M. W. (2012). Tin oxide with controlled morphology and crystallinity by atomic layer deposition onto graphene nanosheets for enhanced lithium storage. Advanced Functional Materials, 22(8), 1647-1654

[27] Chetri, P., & Choudhury, A. (2015). Investigation of structural and magnetic properties of nanoscale Cu doped SnO_2: an experimental and density functional study. Journal of Alloys and Compounds, 627, 261-267.

[28] Babu, B., Reddy, C. V., Shim, J., Ravikumar, R. V. S. S. N., & Park, J. (2016). Effect of cobalt concentration on morphology of Co-doped SnO_2 nanostructures synthesized by solution combustion method. Journal of Materials Science: Materials in Electronics, 27(5), 5197-5203.

[29] Zhuang, S., Xu, X., Pang, Y., Li, H., Yu, B., & Hu, J. (2013). Variation of structural, optical, and magnetic properties with Co-doping in $Sn_{1-x}Co_xO_2$ nanoparticles. Journal of Magnetism and magnetic materials, 327, 24-27.

[30] Liu, B., Wang, X., Cai, G., Wen, L., Song, Y., & Zhao, X. (2009). Low-temperature fabrication of V-doped TiO_2 nanoparticles, structure, and photocatalytic studies. Journal of hazardous materials, 169(1-3), 1112-1118.
[31] Sakuma, J., Nomura, K., Barrero, C., & Takeda, M. (2007). Mössbauer studies and magnetic properties of SnO_2 doped with 57Fe. Thin Solid Films, 515(24), 8653-8655.
[32] Toloman, D., Popa, A., Raita, O., Stan, M., Suciu, R., Miclaus, M. O., & Biris, A. R. (2014). Luminescent properties of vanadium-doped SnO_2 nanoparticles. Optical Materials, 37, 223-228.
[33] Letifi, H., Litaiem, Y., Dridi, D., Ammar, S., & Chtourou, R. (2019). Enhanced photocatalytic activity of vanadium-doped SnO_2 nanoparticles in rhodamine B degradation. Advances in Condensed Matter Physics, 2019.
[34] Shume, W. M., Murthy, H. C., & Zereffa, E. A. (2020). A review on synthesis and characterization of Ag_2O nanoparticles for photocatalytic applications. Journal of Chemistry, Article ID 5039479, 15 pages, https://doi.org/10.1155/2020/5039479.
[35] Marimuthu, S., Antonisamy, A. J., Malayandi, S., Rajendran, K., Tsai, P. C., Pugazhendhi, A., & Ponnusamy, V. K. (2020). Silver nanoparticles in dye effluent treatment: A review on synthesis, treatment methods, mechanisms, photocatalytic degradation, toxic effects and mitigation of toxicity. Journal of Photochemistry and Photobiology B: Biology, 205, 111823.
[36] Asaithambi, S., Sakthivel, P., Karuppaiah, M., Murugan, R., Yuvakkumar, R., & Ravi, G. (2019). Preparation of SnO_2 nanoparticles with the addition of Co ions for the photocatalytic activity of brilliant green dye degradation. Journal of Electronic Materials, 48(4), 2183-2194.
[37] Sakwises, L., Pisitsak, P., Manuspiya, H., & Ummartyotin, S. (2017). Effect of Mn-substituted SnO_2 particle toward photocatalytic degradation of methylene blue dye. Results in Physics, 7, 1751-1759.
[38] Kumar, V., Govind, A., & Nagarajan, R. (2011). Optical and photocatalytic properties of heavily F-doped SnO_2 nanocrystals by a novel single-source precursor approach. Inorganic chemistry, 50(12), 5637-5645.
[39] Kumar, V., Govind, A., & Nagarajan, R. (2011). Optical and photocatalytic properties of heavily F-doped SnO_2 nanocrystals by a novel single-source precursor approach. Inorganic chemistry, 50(12), 5637-5645.
[40] You, H., Liu, R., Liang, C., Yang, S., Wang, F., Lu, X., & Ding, B. (2013). Gold nanoparticle doped hollow SnO_2 supersymmetric nanostructures for improved photocatalysis. Journal of Materials Chemistry A, 1(12), 4097-4104.
[41] Wu, W., Liao, L., Zhang, S., Zhou, J., Xiao, X., Ren, F., & Jiang, C. (2013). Non-centrosymmetric Au–SnO_2 hybrid nanostructures with strong localization of plasmonic for enhanced photocatalysis application. Nanoscale, 5(12), 5628-5636..
[42] Davis, M., Hung-Low, F., Hikal, W. M., & Hope-Weeks, L. J. (2013). Enhanced photocatalytic performance of Fe-doped SnO_2 nano architectures under UV irradiation: synthesis and activity. Journal of Materials Science, 48(18), 6404-6409.
[43] Ansari, S. A., Khan, M. M., Ansari, M. O., Lee, J., & Cho, M. H. (2014). Visible light-driven photocatalytic and photoelectrochemical studies of Ag–SnO_2 nanocomposites synthesized using an electrochemically active biofilm. RSC advances, 4(49), 26013-26021.
[44] Toloman, D., Popa, A., Raita, O., Stan, M., Suciu, R., Miclaus, M. O., & Biris, A. R. (2014). Luminescent properties of vanadium-doped SnO_2 nanoparticles. Optical Materials, 37, 223-228.
[45] Ran, L., Zhao, D., Gao, X., & Yin, L. (2015). Highly crystalline Ti-doped SnO_2 hollow structured photocatalyst with enhanced photocatalytic activity for degradation of organic dyes. CrystEngComm, 17(22), 4225-4237.
[46] Zhao, Q., Deng, X., Ding, M., Gan, L., Zhai, T., & Xu, X. (2015). One-pot synthesis of Zn-doped SnO_2 nanosheet-based hierarchical architectures as a glycol gas sensor and photocatalyst. CrystEngComm, 17(23), 4394-4401.
[47] Khan, M. M., Ansari, S. A., Khan, M. E., Ansari, M. O., Min, B. K., & Cho, M. H. (2015). Visible light-induced enhanced photoelectrochemical and photocatalytic studies of gold decorated SnO_2 nanostructures. New Journal of Chemistry, 39(4), 2758-2766.
[48] Chandran, D., Nair, L. S., Balachandran, S., Babu, K. R., & Deepa, M. (2015). Structural, optical, photocatalytic, and antimicrobial activities of cobalt-doped tin oxide nanoparticles. Journal of Sol-Gel Science and Technology, 76(3), 582-591.
[49] Sivakarthik, P., Thangaraj, V., Perumalraj, K., & Balaji, J. (2016). Synthesis of co-doped tin oxide nanoparticles for photo catalytic degradation of synthetic organic dyes. digest journal of nanomaterials and biostructures, 11(3), 935-943.

[50] Mani, R., Vivekanandan, K., & Vallalperuman, K. (2017). Synthesis of pure and cobalt (Co) doped SnO_2 nanoparticles and its structural, optical and photocatalytic properties. Journal of Materials Science: Materials in Electronics, 28(5), 4396-4402.
[51] Ben Haj Othmen, W., Sieber, B., CORDIER, C., Elhouichet, H., Addad, A., Gelloz, B., & Boukherroub, R. (2016). Iron addition induced tunable band gap and tetravalent Fe ion in hydrothermally prepared SnO_2 nanocrystals: Application in photocatalysis, Materials Research Bulletin,83, 481-490.
[52] Soltan, W. B., Mbarki, M., Ammar, S., Babot, O., & Toupance, T. (2016). Structural and optical properties of vanadium doped SnO_2 nanoparticles synthesized by the polyol method. Optical Materials, 54, 139-146.
[53] Sinha, T., & Ahmaruzzaman, M. (2016). Indigenous north eastern India fern mediated fabrication of spherical silver and anisotropic gold nano structured materials and their efficacy for the abatement of perilous organic compounds from waste water-A green approach. RSC advances, 6(25), 21076-21089.
[54] Nasir, Z., Shakir, M., Wahab, R., Shoeb, M., Alam, P., Khan, R. H., & Mobin, M. (2017). Co-precipitation synthesis and characterization of Co doped SnO_2 NPs, HSA interaction via various spectroscopic techniques and their antimicrobial and photocatalytic activities. International journal of biological macromolecules, 94, 554-565.
[55] Qamar, M. A., Shahid, S., Khan, S. A., Zaman, S., & Sarwar, M. N. (2017). Synthesis characterization, optical and antibacterial studies of Co-doped SnO_2 nanoparticles. Dig J Nanomater Biostruct, 12(4), 1127-1135.
[56] Karpuraranjith, M., & Thambidurai, S. (2017). Hybrid structure of biotemplate-zinc-tin oxide for better optical, morphological and photocatalytic properties. Semiconductor Science and Technology, 32(3), 035014.
[57] Mala, N., Ravichandran, K., Pandiarajan, S., Srinivasan, N., Ravikumar, B., & Nithiyadevi, K. (2017). Enhanced antibacterial and photocatalytic activity of (Mg+Co) doped tin oxide nanopowders synthesised using wet chemical route. Materials technology, 32(11), 686-694.
[58] Sakwises, L., Pisitsak, P., Manuspiya, H., & Ummartyotin, S. (2017). Effect of Mn-substituted SnO_2 particle toward photocatalytic degradation of methylene blue dye. Results in Physics, 7, 1751-1759.
[59] Bhuvaneswari, K., Bharathi, R. D., & Pazhanivel, T. (2018). Silk fibroin linked Zn/Cd-doped SnO_2 nanoparticles to purify the organically polluted water. Materials Research Express, 5(2), 024004.
[60] Babu, B., Kadam, A. N., Rao, G. T., Lee, S. W., Byon, C., & Shim, J. (2018). Enhancement of visible-light-driven photoresponse of Mn-doped SnO_2 quantum dots obtained by rapid and energy efficient synthesis. Journal of Luminescence, 195, 283-289.
[61] Asaithambi, S., Sakthivel, P., Karuppaiah, M., Murugan, R., Yuvakkumar, R., & Ravi, G. (2019). Preparation of SnO_2 nanoparticles with addition of co ions for photocatalytic activity of brilliant green dye degradation. *Journal of Electronic Materials*, *48*(4), 2183-2194.
[62] Sujatha, K., Seethalakshmi, T., Sudha, A. P., & Shanmugasundaram, O. L. (2019). Photocatalytic activity of pure, Zn doped and surfactants assisted Zn doped SnO_2 nanoparticles for degradation of cationic dye. Nano-Structures & Nano-Objects, 18, 100305.
[63] Letifi, H., Litaiem, Y., Dridi, D., Ammar, S., & Chtourou, R. (2019). Enhanced photocatalytic activity of vanadium-doped SnO_2 nanoparticles in rhodamine B degradation. Advances in Condensed Matter Physics, Article ID 2157428, 11 pages, https://doi.org 1155/2019/2157428.
[64] Sathishkumar, M., & Geethalakshmi, S. (2020). Enhanced photocatalytic and antibacterial activity of Cu: SnO_2 nanoparticles synthesized by microwave assisted method. Materials Today: Proceedings, 20, 54-63.
[65] Sujatha, K., Seethalakshmi, T., Sudha, A. P., & Shanmugasundaram, O. L. (2020). Photoluminescence properties of pure, Fe-doped and surfactant-assisted Fe-doped tin-oxide nanoparticles. Bulletin of Materials Science, 43(1), 1-10.
[66] Ali Baig, A. B., Rathinam, V., & Ramya, V. (2021). Synthesis and investigation of Fe-doped SnO_2 nanoparticles for improved photocatalytic activity under visible light and antibacterial performances. Materials Technology, 36(10), 623-635.
[67] Wang, Q., Tian, J., Wei, L., Liu, Y., & Yang, C. (2020). Z-scheme heterostructure of Fe-doped SnO_2 decorated layered g-C3N4 with enhanced photocatalytic activity under simulated solar light irradiation. Optical Materials, 101, 109769.
[68] Ramamoorthy, M., Ragupathy, S., Sakthi, D., Arun, V., & Kannadasan, N. (2020). Enhanced sunlight photodegradation activity of methylene blue using Mn doped SnO_2 loaded on corn cob activated carbon. Results in Materials, 8, 100144.
[69] Suthakaran, S., Dhanapandian, S., Krishnakumar, N., Ponpandian, N., Dhamodharan, P., & Anandan, M. (2020). Surfactant-assisted hydrothermal synthesis of Zr doped SnO_2 nanoparticles with photocatalytic and supercapacitor applications. Materials Science in Semiconductor Processing, 111, 104982.

[70] Baig, A. B. A., Rathinam, V., & Palaninathan, J. (2020). Fabrication of Zr-doped SnO_2 nanoparticles with synergistic influence for improved visible-light photocatalytic action and antibacterial performance. Applied Water Science, 10(2), 1-12.

[71] Baig, A. B. A., Rathinam, V., & Palaninathan, J. (2020). Photodegradation activity of yttrium-doped SnO_2 nanoparticles against methylene blue dye and antibacterial effects. Applied Water Science, 10(2), 1-13.

[72] Carolin, L. R., & Samuel, S. S. A. (2020). Hierarchical nanostructures of In–SnO_2 with enhanced photocatalytic activity for the degradation of RR 120 dye. Journal of Materials Science: Materials in Electronics, 31(15), 12796-12806.

[73] Chu, L., Duo, F., Zhang, M., Wu, Z., Sun, Y., Wang, C., & Sun, J. (2020). Doping induced enhanced photocatalytic performance of SnO_2: Bi^{3+} quantum dots toward organic pollutants. Colloids and Surfaces A: Physicochemical and Engineering Aspects, 589, 124416.

[74] , P. Kathirvel1, D. Maruthamani , S.D. Gopal Ram, . Sivarama Prabhu P (2021). Synthesis of SnO_2 and Zn doped SnO_2 Nanoparticles by Flame Oxidation Process for photocatalytic degradation of Methylene Blue dye, Research Square under review

[75] Salah Ud Din, Sabah Hanif Kiani , Sirajul Haq , Pervaiz Ahmad, Mayeen Uddin Khandaker , Mohammad Rashed Iqbal Faruque , Abubakr M. Idris and M. I. Sayyed (2022), Bio-Synthesized Tin Oxide Nanoparticles: Structural, Optical, and Biological Studies in Crystals , 12, 614, pp 1-12.